ORIGINAL PAPER

INSIGHTS ON CHARACTERIZATION AND CONSERVATION OF THE GLAZED INKWELL FROM THE UMAYYAD PERIOD, ROSETTA, EGYPT

RANIA ABDEL GWAD ELORIBY[1]

Manuscript received: 21.01.2026; Accepted paper: 15.03.2026;
Published online: 30.03.2026.

Abstract. *This research examines a glazed inkwell from the Umayyad era preserved in the Rosetta store of antiquities. It was discovered during excavations at Tell Abu Mandour in the 2022-2023 season. The study also seeks to characterise the artefact's chemical composition, identify its components in both the glaze layer and the fired clay body, and diagnose signs of deterioration. Therefore, the inkwell was documented using AutoCAD, and a multi-analytical approach was used to investigate the inkwell through stereomicroscopy, polarised light microscopy (PLM), scanning electron microscopy coupled with energy dispersive X-ray spectroscopy (SEM-EDX), X-ray diffraction (XRD), thermal analysis, and Fourier transform infrared spectroscopy (FTIR). The results of microscopic examination revealed that the surface of the glaze layer had cracks, missing parts, accumulated dirt, peeling, and flaking. The polarised microscope indicated that the glazed inkwell consisted of three layers: the glaze, slip, and fired clay body. EDX confirmed the presence of a lead-based glaze containing manganese, copper, and iron colouring agents. XRD revealed the presence of quartz, gehlenite, and diopside, thereby confirming a calcareous clay body. FTIR spectroscopy indicated that gum Arabic was used to fix the decorations within the glaze layer. In addition, thermal analysis revealed that the clay body's firing temperature ranged from 850 °C to 900°C. Finally, the treatment and restoration processes were carried out, comprising cleaning, completion, and consolidation to preserve its artistic and archaeological value and protect it from further damage and deterioration.*

Keywords: *Glaze layer; inkwell; Umayyad period; deterioration; SEM-EDX; conservation.*

1. INTRODUCTION

In early Islamic applied arts, writing tools, especially inkwells, played a key role as literacy grew in importance. Muslim artisans focused on shaping and decorating these implements, employing advanced glazing techniques [1,2]. The glaze is crucial for enhancing the artistic and aesthetic qualities of ceramic objects. It also seals the pores, makes cleaning easier, and gives the pieces a smooth, glossy finish [3,4]. The glaze layer is made of silica as the main glazing agent, along with fluxes, stabilising agents, and colourants. During firing, these materials fuse to create the glaze [5,6].

Glazes are categorised into three types based on the flux: alkaline, lead, and alkali-lead glazes [7,8]. Lead glaze was common from late Roman times and became especially widespread during the Umayyad period (661-750 CE) as a vital element of early Islamic art

[1] Cairo University, Faculty of Archaeology, Department of Inorganic Materials Conservation, 12613 Giza, Egypt. E-mail: rania88@cu.edu.eg

https://doi.org/10.46939/J.Sci.Arts-26.1-b05

[9,10]. The Umayyad glaze decoration featured several artistic styles and characteristics. It started as plain but later incorporated geometric and floral patterns, as well as Kufic script [11,12]. Glaze colours were limited to brown, green, and yellow, and sometimes a transparent glaze was used to highlight the designs. Techniques such as engraving and relief carving were employed to add unique ornaments beneath the glaze layers [13,14].

However, the stability and durability of these layers rely heavily on the thermal compatibility between the glaze and the clay body, particularly their expansion and contraction coefficients. Any mismatch can cause internal stresses, leading to hairline cracks, crazing, flaking, and separation. The burial environment also plays a significant role in worsening these stresses, causing serious damage [15,16].

The glazed inkwell studied was excavated at Tell Abu Mandour in Rosetta during the 2022-2023 season. The site is located on the Rosetta branch of the Nile, with an elevation of 15-18 meters, covering an area of 52 acres, and measuring 720 meters long and 250 meters wide (Fig. 1a, b). It consists of a series of sandy mounds that give the location a prominent topography, gradually decreasing toward the western side of the Nile [17,18].

Although the discovery of the inkwell in the sandy layers of these mounds spared it from severe mechanical stress, the proximity to the riverbank and fluctuating weather conditions exposed the glaze to continuous cycles of wetting and drying [19,20]. The sand's high porosity allowed moisture and dissolved salts to infiltrate the glaze's microcracks, causing erosion and flaking at the interface with the clay body [21]. Additionally, the relative humidity in the coastal environment promotes ion exchange between hydrogen ions in the environment and alkali ions in the glaze, weakening the glaze's structure and promoting surface corrosion [22-24].

Therefore, this research aims to analyse this glazed inkwell, determine the chemical compositions of both the glaze and the fired clay, and investigate the causes of its deterioration. Furthermore, the study seeks to develop a treatment and conservation plan for the inkwell, including cleaning, completion, and consolidation, to prevent further damage given its important archaeological and artistic significance.

(a) (b)

Figure 1. (a) Location of Tell Abu Mandour; (b) Tell Abu Mandour excavation site.

2. MATERIALS AND METHODS

2.1. DESCRIPTION OF GLAZED INKWELL

The glazed inkwell under study is kept in the Rosetta store of antiquities under number 929. Its dimensions are 13 cm by 13 cm. In the centre of the inkwell is a circular pouch surrounded by three dark brown circles. Each of its four corners forms an almond shape in brown, and between them are writings in leafy Kufic script that read (Omar - for Egypt - the era - to Egypt). The inkwell is surrounded by a frame of hatchings and touching beads in brown. The reverse side of the inkwell is undecorated and features four protrusions that form its base. It dates to the Umayyad period (1^{st} century AH / 7^{th} century CE).

2.2. VISUAL ASSESSMENT

Sony Cyber-shot DSC-HX10V compact camera (Sony Group Corporation, Tokyo, Japan) was used for examination of the glazed inkwell. The features of the camera include a 25 mm wide-angle lens (35 mm format), suitable for capturing wide images, full HD (1920 x 1080) movie recording, 16x Clear Image Zoom, and a 16 mm Exmor R CMOS sensor with 8X optical zoom.

2.3. AUTOCAD DOCUMENTATION

The documentation produced using the AutoCAD program indicated that the glazed inkwell exhibited some features in a deteriorating state.

2.4. STEREO MICROSCOPY

A stereomicroscope is one of the most important instruments, providing three-dimensional images of the surface that greatly aid in assessing and identifying signs of deterioration [25]. A Leica MZ6 stereo zoom microscope (Leica Microsystems GmbH, Wetzlar, Germany), with a magnification range of 6.3x to 40x, was used. This process was carried out at the General Authority of Metallic Resources in Dokki, Cairo, Egypt.

2.5. POLARISED MICROSCOPY

Polarised microscopy (PLM) was used to investigate the mineral appearance and texture in the specimens [26]. The samples were subjected to thin-section procedures, and the polarised microscope was a Nikon Eclipse LV 100 POL Polarizing Light Microscope, with Nikon DS-Fi1 digital camera (Nikon, Tokyo, Japan). The utilised PLM is at the Department of Geology, the Faculty of Science, Cairo University, Egypt.

2.6. SCANNING ELECTRON MICROSCOPY - ENERGY DISPERSIVE X-RAY SPECTROSCOPY

Scanning Electron Microscopy-Energy Dispersive X-ray Spectroscopy (SEM-EDX) was used to study the exterior of the glazed inkwell. This system provides precise information on durability, surface deposition layers, pits, scratches, fissures, and cracks [27]. The investigation was performed using a Quanta 250 FEG device (FEI Corporation, Eindhoven, Netherlands) coupled with EDX with a higher voltage of 30 kV, 14x magnification up to 1,000,000, and a gun resolution of 1 nm. This was performed in the SEM Laboratory of the Egyptian Mineral Resources Authority in Dokki, Egypt.

2.7. X-RAY DIFFRACTION

X-ray diffraction (XRD) was used to analyse the glaze layer and the fired clay body. The XRD analysis was conducted using the D8 Advance equipment (Bruker, Billerica, MA, United States), which provides reflectometry, high-resolution diffraction, in-plane grazing incidence diffraction (IP-GID), and small-angle X-ray scattering (SAXS) analysis. This was analyzed at the Egyptian Centre of Nanotechnology in Sheikh Zayed, Egypt, affiliated with Cairo University.

2.8. DERIVATIVE THERMOGRAVIMETRY

Derivative thermogravimetry (DTG) is the derivative of the thermogravimetric analysis (TGA) curve and differential thermal analysis (DTA), representing the rate of mass change (*dm/dt* or *dm/dT*) with respect to time or temperature. DTG analyses were performed using a DTG-60 H Shimadzu (max. 1,500 °C) system (Shimadzu, Tokyo, Japan) in a nitrogen atmosphere in Japan. This analysis was performed at the Microanalysis Centre, Faculty of Science, Cairo University, Egypt.

2.9. FOURIER TRANSFORM INFRARED SPECTROSCOPY

The analysis was carried out at the Microanalytical Centre, Faculty of Science, Cairo University, Egypt, using the JASCO 460 plus FTIR spectrometer (Jasco, Tokyo, Japan) over the range 400-4000 cm^{-1}. The procedure is typically employed to determine the chemical characterisation of coloured materials and to characterise organic and inorganic materials with varying degrees of infrared absorption by detecting the functional groups of each compound [28].

3. RESULTS AND DISCUSSION

3.1. PHYSICOCHEMICAL CHARACTERIZATION

The visual examination reveals several signs of damage in the glazed inkwell, including loss of a part at one edge, flaking, and peeling of the glaze layer in various locations. cracks and fissures are present on the surface of the glaze (Fig. 2). Although the surface shows several signs of deterioration, the object is generally in fair condition, as the fired clay body remains partially cohesive. This may be attributed to the burial environment before its discovery in excavations, which was sandy and thus helped preserve the object to a large extent in its current state.

Figure 2. Studied glazed inkwell.

The dimensions of the glazed inkwell were confirmed and documented using AutoCAD. It is used to accurately map various forms of deterioration observed on the inkwell (Fig. 3).

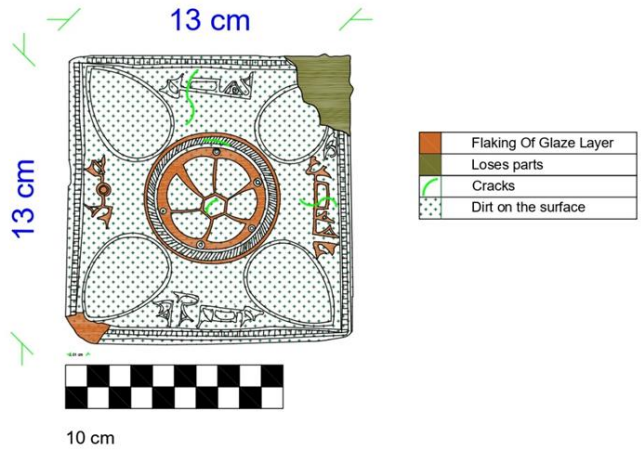

Figure 3. Documentation of the glazed inkwell using AutoCAD.

The examination under the stereo microscope showed that the surface of the brown glaze exhibits crazing (Fig. 4a). Crazing mostly occurs because of the tensile strength in the glaze material and the disparity in the expansion and contraction between the body and the applied glaze. Also, the tensile stress associated with the mismatch between the contracting

glaze layer and the body leads to crazing and the loss of the glaze layer or portions of it during cooling. As tensile stress increases, the glaze layer begins to flake and eventually separates. In addition, the use of a thick glaze layer on the body contributes to differences in the expansion and contraction coefficients between the glaze layer and the body [29]. Furthermore, the crystallisation of salt within the body is one of the causes of the flaking and separation of the glaze layer. Given the nature of the previously mentioned discovery site, the porosity of the sandy soil allows dissolved salt solutions to pass through the microcracks in the glaze layer. As the soil dries, these salts crystallise, generating mechanical pressures that push against the glaze, causing it to detach as flaking layers.

Additionally, the dark brown glaze exhibited pits on the surface (Fig. 4b). These pits are small gas bubbles that form during firing, penetrate the glaze, and explode on the surface, leaving pits behind [30]. It is also observed that the dark green glaze showed air bubbles on the surface (Fig. 4c). Air bubbles result from insufficient melting of the glaze on the body and the failure to release trapped gases. These bubbles detract from the appearance and transparency of the glaze layer and weaken its durability [31]. Accumulation of dirt and dust is noticeable on the green glaze surface (Fig. 4d). Moreover, crazing occurs on the green glaze (Fig. 4e). Furthermore, the inkwell body shows a reddish color (Fig. 4f) Therefore, in the past, craftsmen applied a slip layer to hide the defects and color of the body, and to make the glazing layer more prominent [32].

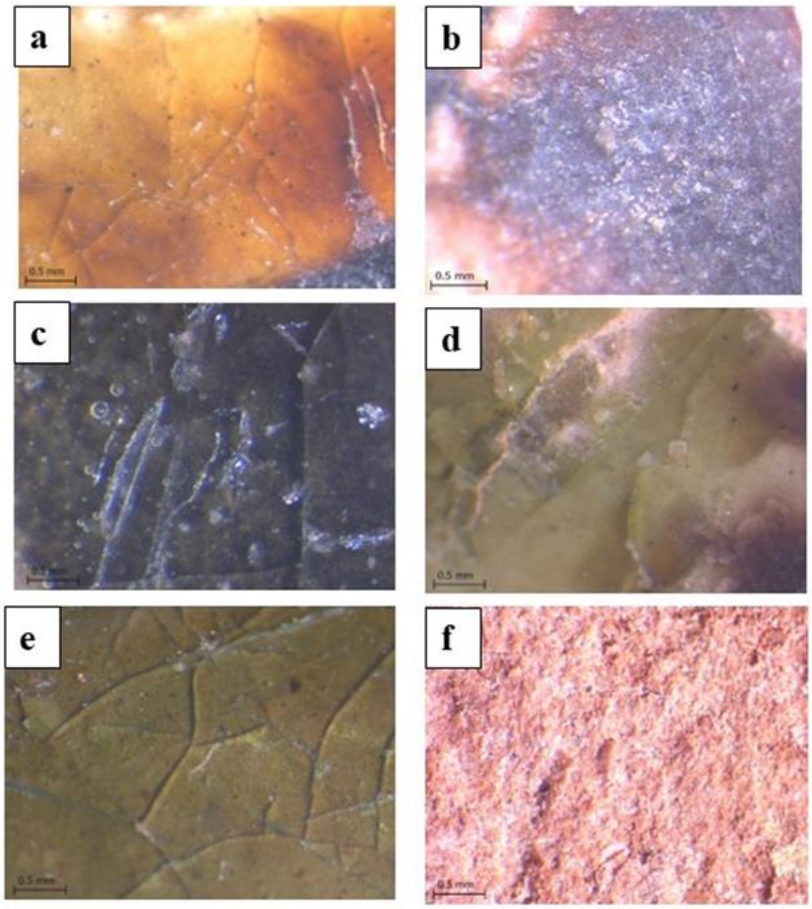

Figure 4. Stereo microscope examination (a) microcracks of the brown glaze; (b) pits on dark brown glaze; (c) air bubbles on the dark green glaze; (d) accumulation of deposited layers of dust and dirt on the surface of the glaze layer; (e) microcracks on the surface of green glaze layer; (f) the texture of the fired clay body.

Petrographic study with a polarised microscope is significant because it enables precise examination of the optical characteristics of the minerals in the sample. It is applicable in the study of the mineral compositions that constitute the fired clay body, grain size, and surface structure, using the arrangement, size, and shape of the grains. It can also verify the existence of the slip layer and examine the correlation between the body and the glaze layer [33].

Cross sections of the brown glaze and the body are shown in Fig. 5 (a-d). These micrographs reveal the three layers of the sample: the glaze, the slip, and the body. The body fabric consists of a fired clay matrix in which some quartz grains are large and visible, while others are smaller. The slip layer has a kaolin clay texture and consists of small, subrounded quartz grains. A distinct interface is also visible between the body and the slip, with no overlap between the two layers (Fig. 5c, d). This may suggest that the sample underwent two firing stages: one for the body and another for the slip [34]. The texture of the body indicates a semi-homogeneous, fine-grained clay matrix with quartz grains of varying sizes scattered throughout, along with occasional large particles and dark-coloured iron oxides (Fig. 5e, f).

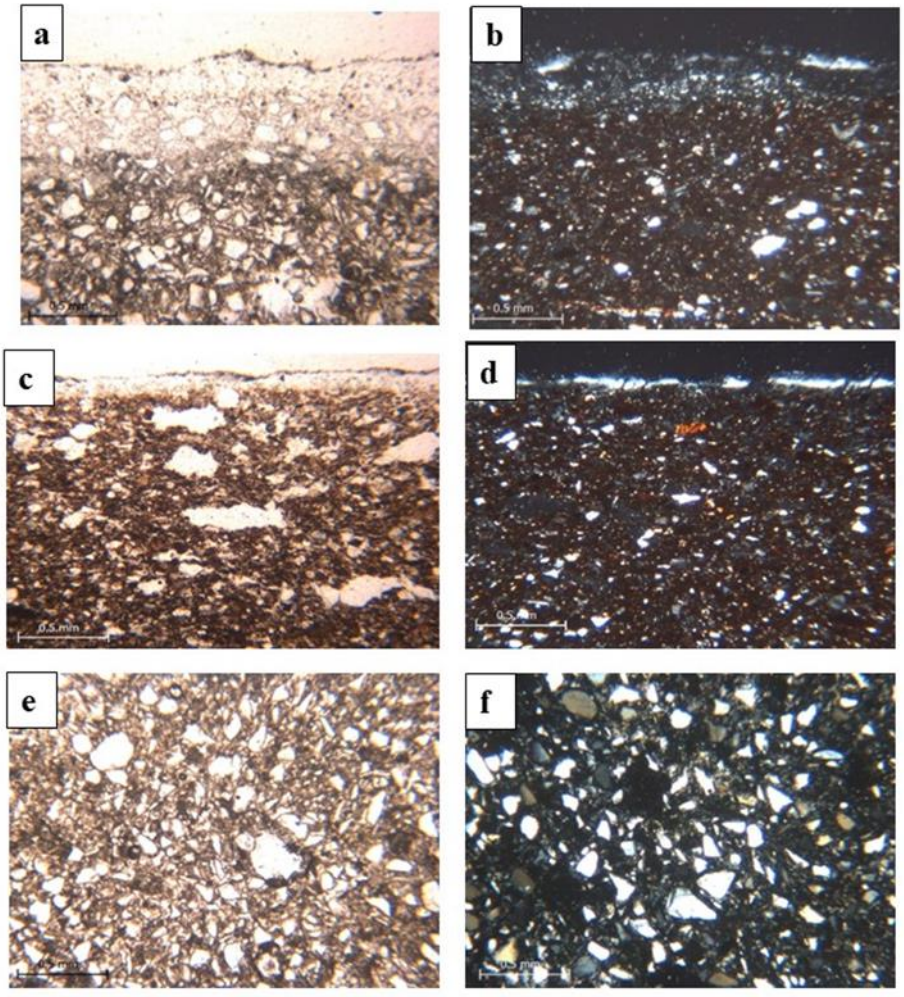

Figure 5. Polarised micrographs (a, c, e) P.L., (b, d, f) C.N., (a, b, c, d) cross sections of the brown glaze, slip, and fired clay body (a, b) with three layers; (c, d) the distribution of the quartz and the interface; (e, f) the fired clay body fabric.

The SEM method is extensively used to examine the morphology of the samples and evaluate the surface appearance of the glazed samples and the fired clay body. The brown-

glazed sample (Fig. 6a) shows cracks and fissures on its surface. The dark brown glaze sample (Fig. 6c) shows the extent of deterioration in the glaze layer, with peeling, delamination, spreading microcracks, and nonuniform distribution of coloured oxide particles. It also shows that the glazing layer is thinner, making the body visible from beneath it. As shown in (Fig. 6e), the green glaze shows evident deterioration, such as flaking, corrosion of the surface, and pores. The body texture appears semi-homogeneous of the fired clay components. Quartz grains of uniform and varying sizes are present, embedded within some larger grains (Fig. 6g), corresponding to a polarised light micrograph of a section of the body. Crystallisation of salts is also observed between the grains of the clay.

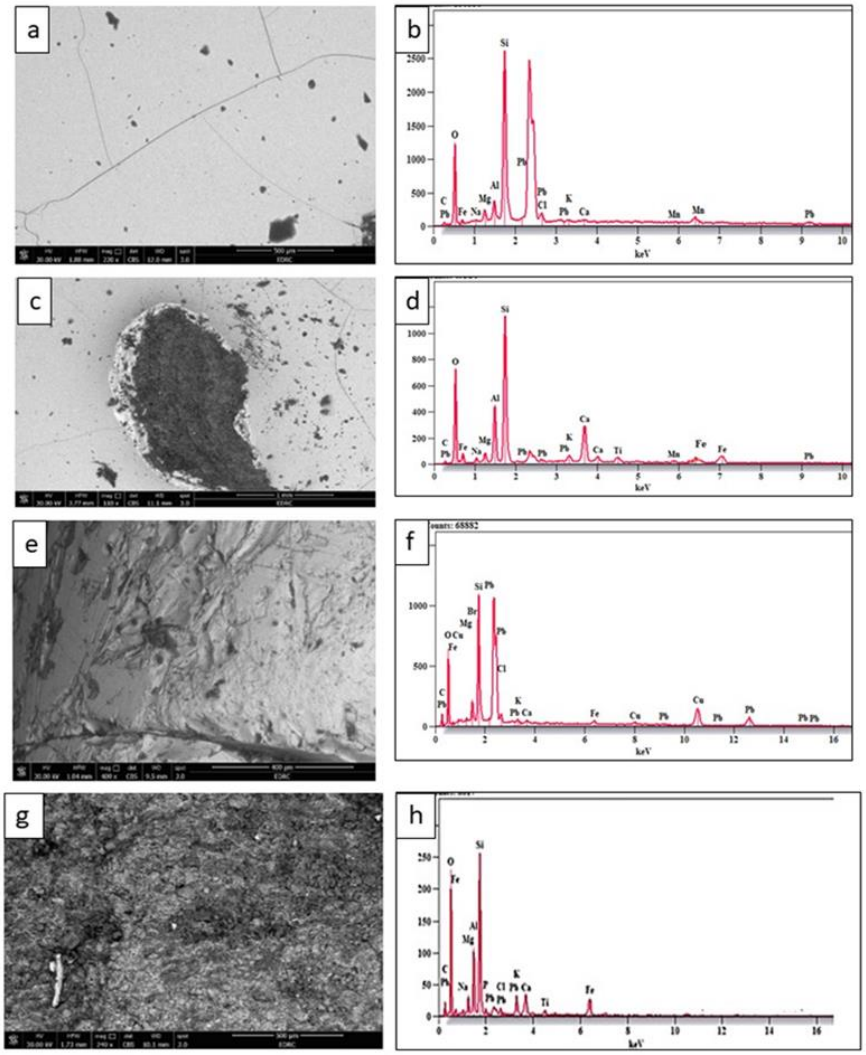

Figure 6. SEM images and EDX spectra of samples (a, b) brown glaze; (c, d) dark brown glaze; (e, f) green glaze; (g, h) fired clay body.

The elemental composition of the glaze layers and the underlying fired clay body was determined by energy-dispersive X-ray (EDX) analysis, and the results are shown in Table 1 and Fig. 6. The results show that the percentage of lead in the coloured glaze layer is higher than that of sodium and potassium. The percentage of lead is 32.8% (avg.), indicating lead oxide as the primary flux agent in the glaze layer. Sodium and potassium concentrations average (4.1%, 1.6%, respectively), indicating that their presence is attributed to use as auxiliary fluxes and to the role in reducing the coating's viscosity. Silica is detected in proportions (avg. 26.23%) and is considered a major component of the glaze layer. However, this percentage is lower than the standard rates of 37-42% [9,10], which is attributed to the

impact of soil moisture in the sandy burial environment that induced silica leaching and chemical degradation.

As shown in the analysis, Aluminum, calcium, and magnesium are also identified. These elements are considered among the primary components of the glaze layer [35]. The observed results are consistent with previous studies [5, 36], indicating the widespread use of lead glazes in the early Islamic period. This is attributed to the ease and simplicity of applying lead glazes to clay bodies compared to alkaline glazes, as lead glazes possess low surface tension and a low coefficient of thermal expansion, which is compatible with fired clay bodies [37]. Furthermore, lead glazes are characterised by high density, transparency, lustre, and excellent optical properties due to their high refractive index [28]. They also exhibit a high capacity for dispersing colouring pigments, are readily available, and are easy to use and fire [38].

The results also show the colouring agents in the glaze layers, such as manganese (1.4%) in the brown glaze, are responsible for the brown colour [39]. Manganese and iron appear at a percentage (2.3% and 1.2% respectively) in the dark brown glaze, contributing to the dark brown colour [40]. Copper appears at a percentage of (1.7%) in the green glaze layer, responsible for the green colour [41]

Moreover, the EDX results show that the fired clay body is composed primarily of silica. The high percentage of calcium in the clay is evident at a percentage (18.3%). This may be due to the addition of a binding agent, resulting from burning the calcium carbonate that is already present in the clay, or it may result from the use of calcareous clay in the manufacture of the body of this inkwell [42]. The reddish colour of the clay is due to the presence of iron oxide at a percentage of (4.3%). The analysis also reveals sodium, magnesium, and aluminium as components of clay [43]. Furthermore, chlorine is detected at (1.2) % due to the absorption of dissolved salts from the burial environment.

Table 1. Percentage of elements in colored glaze samples and fired clay body with EDX.

Sample	Elements [w_t %]												
	C	**O**	**Si**	**Na**	**Ca**	**Mg**	**Al**	**K**	**Fe**	**Pb**	**Mn**	**Cl**	**Cu**
Brown glaze	5.2	23.1	26.2	2.8	2.4	1.8	2.8	1.6	0.5	31.7	1.4	0.5	----
Dark Brown glaze	3.1	21.1	27.8	4.4	----	0.8	1.8	1.7	1.2	35.8	2.3	----	----
Green glaze	7.4	22.9	24.7	5.2	2.3	0.9	1.6	1.1	0.9	30.9	----	0.4	1.7
Fired clay body	5.7	24.8	29.9	3.2	18.3	1.7	9.5	1.4	4.3	----	----	1.2	----

XRD analysis is used to determine the minerals that identify the glaze layer and the fired clay body. It is used with crystalline materials [44]. XRD also helps study changes that occur during firing, which assists in determining the firing temperature, since mineralogical phases change with the firing temperature reached [45]. The sample of the green glaze layer (Fig. 7a) consists of quartz, gehlenite, copper oxide, and lead oxide. Quartz is a crucial component of the glaze layer [46]. The presence of gehlenite indicates that the clay used contains calcite, which was incorporated intentionally to improve its properties [43]. The calcite thermally decomposes between 650 ºC and 900 ºC [47]. Above 800ºC, SiO_2, CaO, and Al_2O_3 combine to yield calcium silicates and calcium aluminium silicates, such as gehlenite and diopside [48]. Copper oxide is responsible for the green colour, while lead oxide acts as a fluxing agent and an essential component in the composition. The brown glaze sample consists of quartz, gehlenite, and manganese oxide, which is responsible for the brown colour (Fig. 7b). The fired clay body (Fig. 7c) consists of quartz, diopside, and hematite. The presence of hematite accounts for the reddish colour of the body. Furthermore, the detection of diopside suggests that the sample underwent effective firing, as it is one of the crystalline phases that appear above 850°C [49].

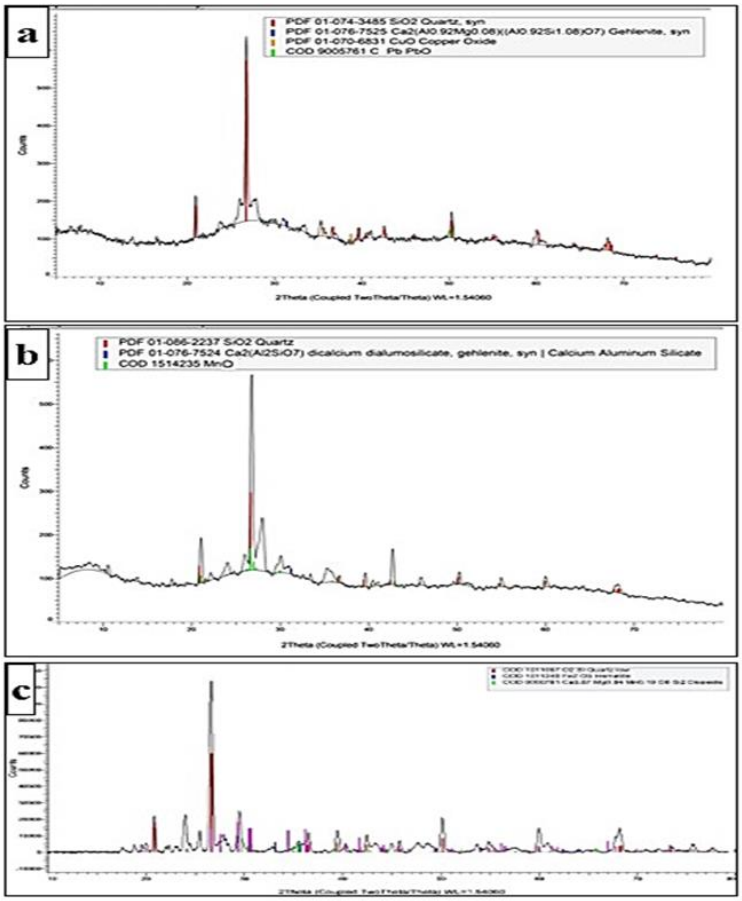

Figure 7. X-ray diffraction pattern of the samples. (a) green glaze; (b) brown glaze; (c) the fired clay body.

The results of (DTG) derivative thermogravimetry, (DTA) differential thermal analysis, and (TGA) thermogravimetric analysis of the fired clay body sample of the inkwell are shown in (Fig 8). DTG converts the transformation of gradual changes in weight into clear peaks that accurately define the temperatures at which the reaction rate is at its maximum (Fig. 8a). The TGA curve (red line) indicates the total mass loss of about 15%, whereas the DTG curve (purple line) shows the reduction by three main stages: the first at 67.32°C, corresponding to the evaporation of physically adsorbed water [50], the second at 611.51°C, indicating the dehydroxylation of clay minerals [51], and the third at 899.40°C, which represents the chemical decomposition of calcium carbonate [52]. This proves that the sample is a calcareous clay that has undergone final structural transformations at high temperatures between 850°C and 900°C.

The DTA curve (Fig. 8.b) indicates that the reaction is endothermic at 50°C due to moisture evaporation, followed by significant thermal activity at higher temperatures, with two distinct endothermic peaks: the first at 823.48°C and the second at 899.63°C. These correspond to the thermal decomposition stage of carbonates (such as calcite), which were observed in the previous DTG curve.

Furthermore, the TGA curve (Fig. 8c) shows a gradual weight loss as temperature increases. At heating temperatures of 31.35°C and 328.03°C, the sample lost 0.197 mg of weight. At temperatures between 516.09°C and 697.64°C, the weight loss of the body sample was 0.083 mg; at temperatures between 870.38°C and 958.14°C, the sample weight decreased by 0.038 mg.

The combined analysis of the TGA, DTG, and DTA curves indicates that the body-firing temperature ranged from 850 °C to 900 °C. These results are consistent with the XRD analysis results due to the presence of minerals gehlenite and diopside.

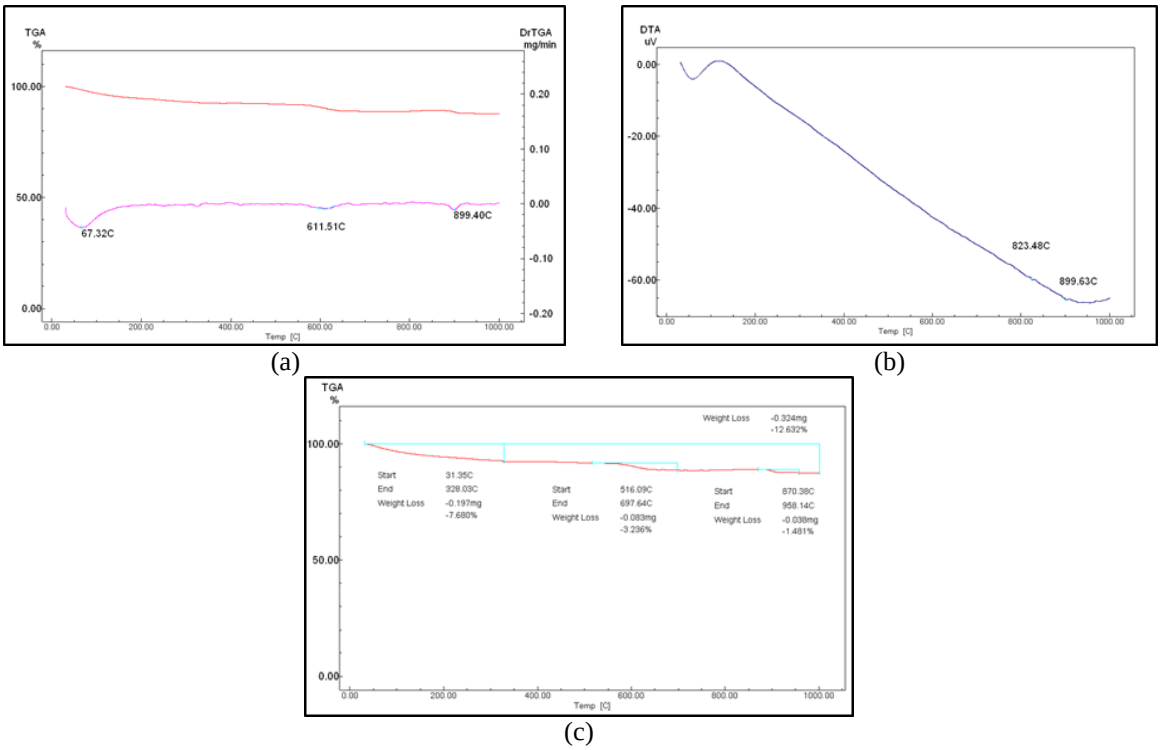

Figure 8. Thermal analysis of the fired clay body of the glazed inkwell (a) DTG curve; (b) DTA; (c) TGA.

The result of FTIR analysis of the green glaze layer (Fig. 9) indicates that gum Arabic was used as a medium to fix the colours on the surface. This is observed in its characteristic functional groups, such as O-H stretching at 3410 cm-1, O-H bending at 1627 cm^{-1}, and C-H bending at 1436 cm^{-1}. In addition, C-O stretching at 1024 cm^{-1} and O-C-O bending bands at 804 cm^{-1} were detected, which overlapped the Si-O-Si and Si-O stretching bands**.** The spectrum also identified the functional groups associated with silica and kaolin, which are the basic components of the fired clay body.

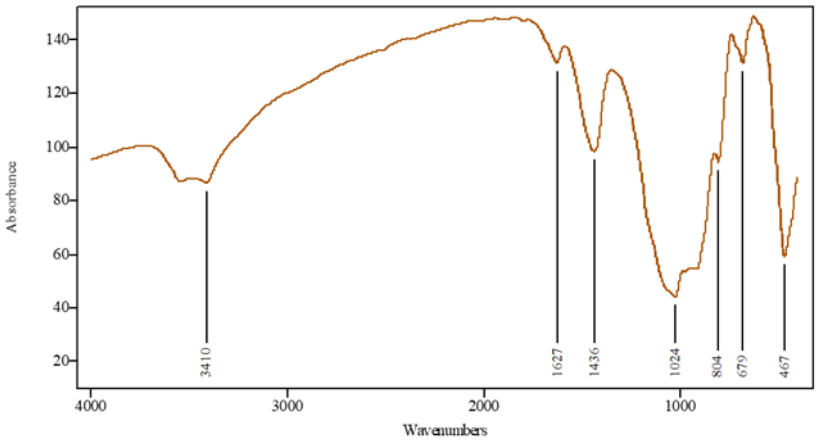

Figure 9. FTIR spectra of the green glaze layer and the body.

3.2. CONSERVATION OF THE GLAZED INKWELL

Cleaning. A mechanical cleaning process was conducted using soft brushes of different degrees of stiffness, as well as using cotton swabs moistened with warm water [53-55], to remove accumulated dust and deposits from the surface of the glazed inkwell (Fig. 10). The procedure was carried out carefully and cautiously to avoid removing or scratching any part of the glaze layer of the artefact.

(a) (b)

Figure 10. (a, b) Mechanical cleaning process of the glazed inkwell.

Completion of the missing part. The completion process can be defined as filling gaps in an artefact by using similar parts based on certain criteria [56]. Completion is important for conserving the durability and stability of the archaeological inkwell and preserving its beauty through the restoration of lost decorations. The missing parts were recreated based on the results of polarised microscopy, which demonstrated a three-layered structure (glaze, slip, and body). Therefore, the reconstruction followed this layered arrangement. The missing body was completed using a mixture of modern reddish pottery powder (Grog), dental plaster, nanotitanium dioxide (TiO_2), and Sika-Bond-LA, diluted 1:1 in distilled water (Fig. 11a). This mixture effectively matched the colour and texture of the original body [57]. To prepare the surface for the decorative elements and the final application of colour, a light-coloured layer simulating the original slip was applied: a mixture of dental plaster, nanotitanium dioxide, and the same solution of Sika-Bond-LA (Fig. 11b).

(a) (b)

Figure 11. Completion of the missing part of the glazed inkwell.

Retouching Process: Inpainting and completion of the glaze decorations. The decorative completion was implemented using tracing paper and then transferred to the correct position. Several experiments were conducted to determine the most suitable colours for retouching the missing parts, including ceramic paints. Specifically, brilliant glossy ceramic (Pebeo) was used in a cold application with its corresponding transparent glaze. Vitrail Le France Bourgeois acrylic paints were also used in cold application, as were Pebeo acrylic paints. These three types of paint are considered among the best for this purpose.

Once the palette of the chosen colours was set, the manual inpainting process was performed to recreate the lost motifs on the glaze layer. The shades were obtained by using fine brushes of different sizes (0, 1, 2, and 3), making them look almost like the original colours but distinguishable when viewed closely. Such careful application had the right effect in the completion of the decorative elements, as shown in (Fig. 12).

(a) (b)

Figure 12. (a) The colours used in the completion of the glaze decorations. (b) Inpainting with fine brushes to complete the glaze motifs.

Consolidation Process. The consolidation process was carried out in the weak areas of the glaze layer. It was performed by injecting the areas of fissures and microcracks, and by using a brush to strengthen the surface of the weak glaze layer. The consolidation was executed using a combination of nanoalumina and nanosilica at 2%, with Silres BS-290 at 7% [58], which proved successful in penetrating the pores and bonding the mineral grains that constitute the inkwell (Fig. 13a, b).

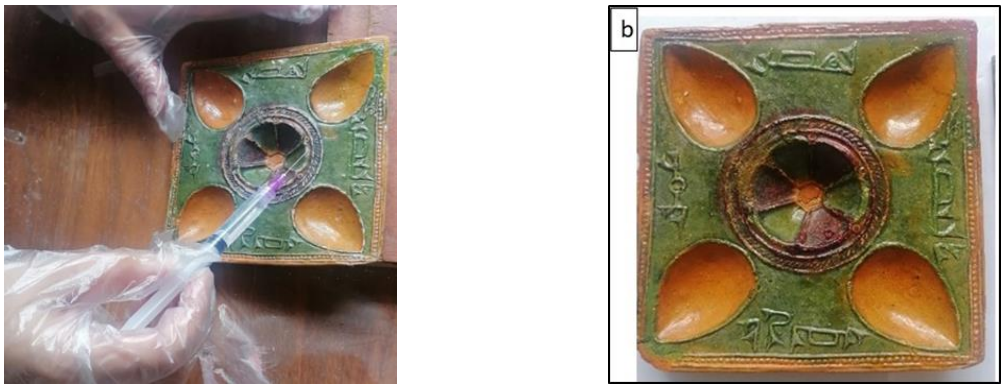

(a) (b)

Figure 13. (a) Consolidation of the weak and flaking glaze layer (b) the glazed inkwell after restoration.

4. CONCLUSIONS

The study of the glazed inkwell preserved in the Rosetta store of antiquities yielded several important results regarding the components of the glaze layer, the body, and the colours used in the glaze. This study helped identify the causes of deterioration and supported the restoration and preservation of the inkwell using modern, appropriate materials. The object was documented using AutoCAD and various microscopies, including a stereomicroscope, polarised light microscopy, and scanning electron microscopy. The examination revealed a weakened glaze layer with fissures, cracks, peeling, and flaking. Polarised light microscopy revealed that the glazed inkwell comprises three layers: the glaze, the slip, and the body. These results facilitated the optimal conservation process.

The EDX analysis provided valuable results about the composition and type of the glaze, the colour oxides, and the body composition. The glaze was determined to be lead-based, with lead oxide as the primary flux (average 32.8%). There was also evidence of alkali presence, with average sodium and potassium contents of 4.1% and 1.6%, respectively, which could be explained by impurities in the raw materials or limited additives used to improve the physical properties of the melt. In the case of the colour oxides, copper oxide was utilised to obtain the green glaze, manganese oxide to obtain the brown glaze, and iron oxide mixed with manganese oxide to obtain the dark brown glaze. The results also revealed that the fired clay body is composed of silica, alumina, and magnesia, the main components of the clay used in its construction, as well as iron oxide, which is responsible for the reddish pink colour of the object.

XRD of the green glaze revealed crystalline phases of quartz, gehlenite, copper oxide, and lead oxide. The brown glaze contained quartz, manganese oxide, and lead oxide. Body analysis showed the presence of quartz, diopside, and iron oxide, which aligns with the EDX results. Gehlenite and diopside indicate a firing temperature of 850-900°C, as confirmed by thermal analysis. FTIR analysis showed that the medium used to fix the decoration was gum Arabic.

The conservation methods began with mechanical cleaning using various brushes to remove dust and dirt from the glaze surface. The procedure was performed with extreme caution due to the fragile structural state of the glaze. Following this, the missing body parts and decorations were addressed. The missing body was filled using a mixture of reddish modern pottery powder (Grog), dental plaster, nanotitanium dioxide (TiO_2), and Sika-Bond-LA diluted 1:1 in distilled water. The preparation layer for re-executing the decorations consisted of dental plaster, TiO_2, and the same Sika-Bond-LA solution, providing a bright white background that accurately reflected the colours and decorations. Acrylic and ceramic paints were used to ensure adequate coverage, and the colours were applied so they could be distinguished from the originals. A compound of nano-alumina and nano-silica at 2%, with Silres BS-290 at 7%, was used to strengthen and protect the glaze against external elements, particularly humidity.

REFERENCES

[1] Vitoa, C. D., Medeghini, L., Mignardi, S., Coletti, F., Contino, A., *Journal of the European Ceramic Society*, **37**, 1779, 2017.
[2] Soslu, A., *Kafkas University Journal of the Institute of Social Sciences*, **30**, 397, 2022.
[3] Ting, C., Lichtenberger, A., Raja, R., *Archaeometry*, **61**(6), 1296, 2019.

[4] Costa, M., Cachim, P., Coroado, J., Rocha, F., Velosa, A., *Materials Science*, **20**(1), 108, 2014.
[5] Al-Saad, Z., *Journal of Archaeological Science*, **29**,803, 2002.
[6] Khamseh, H., Shabani, A. M. R., *Journal of Scientific Research*, **9**(4), 531, 2011.
[7] Meo, Y., *Journal of the American Institute for Conservation*, **39**(2), 195, 2000.
[8] Hatcher, H., Kaczmarczyk, A., Scherer, A., Symonds, R., *American Journal of Archaeology*, **98**(3), 431, 1994
[9] Tite, M. S., Freestone, I., Mason, R., Molera, J., Vendrell-Saz, M., Wood, N., *Archaeometry*, **40**(2), 241, 1998.
[10] Walton, M. S., Tite, M. S., *Archaeometry*, **52**(5), 733, 2010.
[11] Amr, A.J., *Berytus*, **34**, 145, 1986.
[12] Al Gendy, M., *International Design Journal*, **7**(3), 187, 2017.
[13] Rahim, A. N., *Egyptian Journal of Archaeological and Restoration Studies*, **6**(1), 1, 2016.
[14] Walmsley, A., *American Center of Research*, Alexandria, 89, 2022.
[15] Omar, S., Ali, M. F., Ghania, S. A. E., **12**(12), 398, 2024.
[16] Cooper, E., Royle, D., *Glazes for the Studio potter, BT Batsford LTD*, London, 93, 1984.
[17] Jamal, N.A.H., *International Journal of Cultural Inheritance and Social Sciences*, **6**(12), 62, 2024.
[18] Kadir, H., *International Journal of Cultural Inheritance and Social Sciences*, **5**(10), 1, 2023
[19] Fraser, H., *Ceramic faults and their remedies*, A &C BLACK, London, 65, 1986.
[20] Cannillo, V., Esposito, L., Rambaldi, E., Sola, A., Tucci, A., *Journal of the European Ceramic Society*, **29**, 1561, 2009.
[21] Gazulla, M.F., Sánchez, E., González, J.M., and Portillo, M. C., *Journal of the European Ceramic Society*, **31**, 2753, 2011.
[22] Fröberg, L., Hupa, L., Hupa, M., *Journal of the European Ceramic Society*, **29**, 7, 2009.
[23] Eloriby, R. A. G., ELsayed, G. O., Mahmoud, H. I., *Journal of Nano Research*, **82**, 139, 2024.
[24] Carstea (Elekes), A., Gligor, M., Bucurică, I.A., Dulama, I.D., Radulescu, C., Stirbescu, R.M., Stanescu, S.G., Gheboianu, A.I., *Journal of Science and Arts*, **24**(3), 689, 2024.
[25] Filip, D.D., Gligor, M., Lascu, I.A., Bucurica, I.A., Radulescu, C., Stirbescu, R.M., Dulama, I.D., *Romanian Report in Physics*, **77**(2), 803, 2025.
[26] Elghareb, W.K., *International Journal of Conservation Science*, **12**(4), 1327, 2021.
[27] Eloriby, R. A. G., Mohamed, H. M., *Pigment and Resin Technology*, **54**(1), 65, 2025.
[28] Shams, A. H., AlKaradawi, A. S., Eloriby, R. A, *Mediterranean Archaeology and Archaeometry*, **22**, 53, 2022.
[29] Sanders, H., Glazes for Special Effects, Watson-Guptill Publications, NewYork, 14, 1974.
[30] Murfitt, S. T., The Glaze Book, Thames & Hudson, London, 18, 2002.
[31] Eloriby, R., *Egyptian Journal of Archaeological and Restoration Studies*, **11**(2), 176, 2021.
[32] Thomposon, S.J., Glazing, Long Man, U.S.A., 14,1983.
[33] Casale, S., Donner, N., Braekmans, D., Geurds, A., *Microchemical Journal*, **156**, 104829, 2020.
[34] Fabbri, B., Gualtieri, S., Mingazzini, C., Spadea, P., Casadio, P., Costantini, R., Malisani, G., *Archaeometry*, **42**(2), 317, 2000.
[35] Alawneh F., Balaawi F., Alghazaw R., *Conservation Science in Cultural Heritage*, **19**(1), 283, 2019.

[36] Ting, C., Taxel, I., *Archaeological and Anthropological Sciences*, **12**(1), 27, 2020.
[37] Bansal, N. P., Doremus, R. H., Academic Press, New York, 77, 1986.
[38] Cooper, E., Lewenstein, E., Clays and Glazes, Craftsmen Potters Association of Great Britain, 41, 1988.
[39] Khamseh, H. Mirfattah, A., Shabani, R., *Middle-East Journal of Scientific*, **4**, 531, 2011
[40] Chalmin, E., Vignaud, C., Salomon, H., Farges, F., Susini, J., Menu, M., *Applied Physics*, **83**, 213, 2006.
[41] Degeorge, G., Porter, Y., *The Art of the Islamic Tile, Rizzoli International Publications*, United Kingdom, 17, 2002
[42] Mohamed, H. M., *Journal of Science and Arts*, **22**(3), 723, 2022.
[43] Mohamed, H, Omar S., *Spectroscopy Letters*, **56**(7), 364, 2023
[44] Eloriby, R.A.G., *Journal of Science and Arts*, **23**(4), 1019, 2023.
[45] Bersani, D., Lottici, P. P., Virgenti, S., Sodo, A., Malvestuto, G., Botti, A., Salvioli-Mariani, E., Tribaudino, M., Ospital, F., Catarsif, M., *Journal of Raman Spectroscopy*, **41**, 1556, 2010.
[46] Madkour, F., *Egyptian Journal of Archaeological and Restoration Studies*, **4**(1), 13, 2018.
[47] Fabbri, B., Gualtieri, S., Shoval, S., *Journal of the European Ceramic Society*, **34**(7), 1899, 2014
[48] Grammatikakis, I. E., Kyriakidis, E., Demadis, K. D., Diaz, A. C., Leon-Reina, L., *Heritage*, **2**(3), 2652, 2019.
[49] Maritan L., Nodari L., Mazzoli C., Milano A., Russo U., *Applied Clay Science*, **31**, 1, 2006.
[50] Elrahim, E. A., Ahmed, I. I., *Journal of Science and Arts*, **23**(4), 987, 2023.
[51] Chin, C. L., Ahmad, Z. A., Sow, S. S., *Applied Clay Science*, **143**, 327, 2017.
[52] Roy, H., *Transactions of the Indian Ceramic Society*, **23**(1), 181, 2014.
[53] Eloriby, R. A. G., Mohamed, W. S., Mohamed, H. M., *Pigment and Resin Technology*, **54**(3), 434, 2025.
[54] Jammaz, N. H., Ibrahim, M. M., Morgan, N., Eloriby, R., *Egyptian Journal of Chemistry*, **68**(8), 199, 2025.
[55] Jammaz, N. H., Ibrahim, M. M., Eloriby, R. A, Morgan, N., *Journal of Cultural Heritage*, **73**, 73, 2025.
[56] Eloriby, R. A. G., Mohamed, H. A. M., *International Journal of Conservation Science*, **14**(4), 1279, 2023.
[57] Nabil, S., Mohamed, W. S., Ibrahim, M. M., *Egyptian Journal of Chemistry*, **68**(8), 513, 2025.
[58] Eloriby, R. A., Mohamed, W. S., Alkaradawi, A. S., *Mediterranean Archaeology and Archaeometry*, **22**(1) 68, 2022.